High-Performance PML Algorithms

Zhonghua Wu, *Student Member, IEEE*, and Jiayuan Fang, *Member, IEEE*

***Abstract*—This letter presents a revised finite-difference equation, applied at perfectly matched layer (PML) interfaces, that can lead to substantial reduction of numerical reflection from PML absorbers. The properties of the reflection coefficient of PML absorbers implemented with the revised finite-difference equation are studied. The effectiveness of the revised finite-difference equation is verified by numerical tests.**

I. Introduction

THE PERFECTLY matched layer (PML) boundary condition, since its introduction, has received wide acceptance [1]. It has been found that PML is robust to implement and very effective in numerically absorbing outgoing waves.The search for better absorbing boundary conditions, however, has never ended. Recent progresses include the extension of PML to absorb evanescent waves and to be applicable for terminating lossy media [2], [3]. This letter explores the optimum numerical implementation of PML to minimize the numerical reflection.

After numerical discretization of differential equations, the reflection at PML interfaces is no longer zero as it should be in the continuous space [4], [5]. A compromise has to be made on selecting the conductivity profile of a PML absorber. If the conductivity is too small, fields entered into the PML are not sufficiently attenuated and a large reflection is generated at the electric wall terminating the PML absorber and propagates back into the computation domain. If the conductivity of the PML is too large, reflection from medium interfaces becomes significant, which may also end up with a large reflection.

In the finite-difference equation at an interface of two PML media, the material parameters are commonly chosen to be the average of those on two sides of the interface. This letter presents a revised finite-difference equation at PML interfaces. It is found that numerical reflections of PML absorbers with the revised finite-difference algorithm can be much smaller than those with the original algorithm.

II. Derivation of the Revised Finite-Difference Algorithm

For the ease of illustration, the derivation is shown for the two-dimensional (2-D) fields of E_x, E_y, and H_z components. Assume a uniform PML $(\epsilon, \mu, \sigma_{1x}, \sigma_{1x}^*)$, medium 1, in the region $x < 0$ and another uniform PML $(\epsilon, \mu, \sigma_{2x}, \sigma_{2x}^*)$, medium 2, in the region $x > 0$. The interface at $x = 0$ coincides with the electric nodes of E_y. The difference equation for E_y at the interface can be expressed as

$$E_y^{n+1/2}(i, j+1/2) = BE_y^{n-1/2}(i, j+1/2) + C\left[H_z^n(i+1/2, j+1/2) - H_z^n(i-1/2, j+1/2)\right] \quad (1)$$

where B and C are coefficients and can be expressed as

$$B = \frac{\hat{\epsilon}/\Delta t - \hat{\sigma}_x/2}{\hat{\epsilon}/\Delta t + \hat{\sigma}_x/2}, \quad C = -\frac{1}{(\hat{\epsilon}/\Delta t + \hat{\sigma}_x/2)\Delta h} \quad (2)$$

where $\hat{\epsilon}$ and $\hat{\sigma}_x$ in (2) are the material parameters to be determined at the interface. Typically $\hat{\epsilon}$ is chosen as ϵ and $\hat{\sigma}_x$ is chosen to be $(\sigma_{1x} + \sigma_{2x})/2$ [1]–[2].

With the procedure discussed in [5], the numerical reflection coefficient at the interface can be expressed as (3), shown at the bottom of the next page, where Z is defined as E_y/H_z for a plane wave propagating in the $+x$ direction and can be derived as

$$Z = \frac{(\sin(k_{1x}\Delta h/2))/\Delta h}{(\epsilon/\Delta t)\sin(\omega\Delta t/2) - j(\sigma_{1x}/2)\cos(\omega\Delta t/2)} = \frac{(\sin(k_{2x}\Delta h/2))/\Delta h}{(\epsilon/\Delta t)\sin(\omega\Delta t/2) - j(\sigma_{2x}/2)\cos(\omega\Delta t/2)}. \quad (4)$$

The reflection coefficient at the interface for an incident wave coming from medium 2 can be similarly found as (5), also shown at the bottom of the next page.

Next, let us try to determine the values of $\hat{\epsilon}$ and $\hat{\sigma}_x$ to minimize the reflection coefficient R_e in (3). From $\cos(k_{1x}\Delta h/2) = \sqrt{1 - \sin^2(k_{1x}\Delta h/2)}$ and (4), it can be found that

$$\cos(k_{1x}\Delta h/2) \approx \sqrt{1 + (Z\Delta h\sigma_{1x}/2)^2} + j\omega\frac{(Z\Delta h)^2\epsilon\sigma_{1x}}{4\sqrt{1 + (Z\Delta h\sigma_{1x}/2)^2}}. \quad (6)$$

Substitute (6) and the corresponding expression for $\cos(k_{2x}\Delta h/2)$ into the numerator of (3) and let the constant term and the $j\omega$ term in the numerator of (3) be zero. Then, we can get

$$\hat{\sigma}_x = \frac{\sigma_{1x} + \sigma_{2x}}{2} - \sqrt{\left(\frac{1}{Z\Delta h}\right)^2 + \left(\frac{\sigma_{2x}}{2}\right)^2} + \sqrt{\left(\frac{1}{Z\Delta h}\right)^2 + \left(\frac{\sigma_{1x}}{2}\right)^2} \quad (7)$$

$$\hat{\epsilon} = \epsilon - \frac{\epsilon\sigma_{2x}}{4\sqrt{\left(\frac{1}{Z\Delta h}\right)^2 + \left(\frac{\sigma_{2x}}{2}\right)^2}} + \frac{\epsilon\sigma_{1x}}{4\sqrt{\left(\frac{1}{Z\Delta h}\right)^2 + \left(\frac{\sigma_{1x}}{2}\right)^2}} \quad (8)$$

Manuscript received March 20, 1996. This work was supported in part by the National Science Foundation under Contract MIP-9357561 and the Integrated Electronics Engineering Research Center (IEEC) at the State University of New York at Binghamton.

The authors are with the Department of Electrical Engineering, the State University of New York at Binghamton, Binghamton, NY 13902-6000 USA.

Publisher Item Identifier S 1051-8207(96)07059-6.

Note that when $\hat{\epsilon}$ and $\hat{\sigma}_x$ are chosen as (7) and (8), $R_e \neq -R_e^r$. It will be shown that R_e is significantly reduced while R_e^r is slightly increased, and the total reflection of a PML absorber can be substantially reduced with the selection of $\hat{\epsilon}$ and $\hat{\sigma}_x$ as (7) and (8).

With the same procedure, it can be found that when the interface coincides with the magnetic node H_z, the magnetic conductivity $\hat{\sigma}_x^*$ and the permeability $\hat{\mu}$ should be chosen as follows to have the constant and the $j\omega$ terms in the numerator of the reflection coefficient R_h at the interface be zero

$$\hat{\sigma}_x^* = \frac{\sigma_{1x}^* + \sigma_{2x}^*}{2} - \sqrt{\left(\frac{Z}{\Delta h}\right)^2 + \left(\frac{\sigma_{2x}^*}{2}\right)^2} + \sqrt{\left(\frac{Z}{\Delta h}\right)^2 + \left(\frac{\sigma_{1x}^*}{2}\right)^2} \tag{9}$$

$$\hat{\mu} = \mu - \frac{\mu\sigma_{2x}^*}{4\sqrt{\left(\frac{Z}{\Delta h}\right)^2 + \left(\frac{\sigma_{2x}^*}{2}\right)^2}} + \frac{\mu\sigma_{1x}^*}{4\sqrt{\left(\frac{Z}{\Delta h}\right)^2 + \left(\frac{\sigma_{1x}^*}{2}\right)^2}}. \tag{10}$$

The term Z can be approximated as $\eta\cos\theta$, where θ is the incident angle. One can select a particular value of θ to have the PML absorber most effective at that particular incident angle. It will be shown that, by simply choosing Z be η in (7) to (10), the PML absorber is best for the normal incidence but is also generally much better than the original algorithm for other incident angles.

It is apparent that the revised finite-difference equation at PML interfaces, with the material parameters chosen as in (7)–(10), needs no more computer resources than the original scheme.

III. Numerical Tests

The parameters used for the following numerical tests are: $\Delta x = \Delta y = \Delta h = 1$ mm and $\Delta t = 0.5\Delta h\sqrt{\mu\epsilon}$. The parameter θ in the revised finite-difference equation is chosen to be zero unless otherwise stated.

Fig. 1 shows the numerical reflection coefficients R_e and R_e^r for a single interface and at the normal incident angle, with the original and the revised finite-difference implementations. The single interface is of the free space on one side and an uniform PML of $\sigma_x = 1$ S/m on the other side. With the original finite-difference scheme, the magnitude of R_e and R_e^r are the same. With the revised finite-difference scheme, R_e is reduced by a few orders of magnitude and R_e^r is slightly increased.

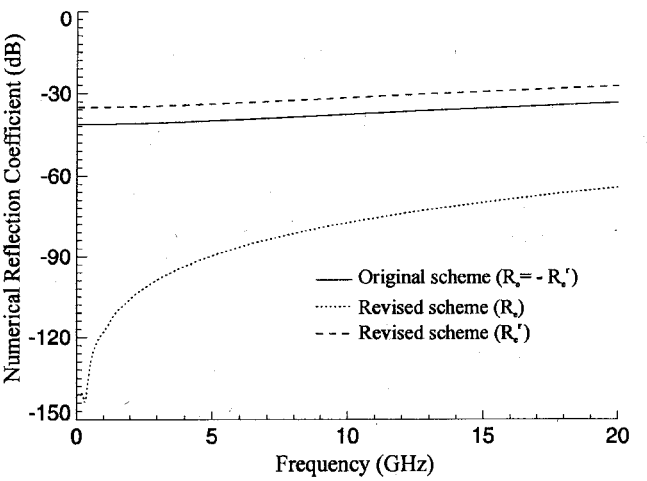

Fig. 1. Numerical reflection coefficients for a single interface with the original and the revised finite-difference equations.

Fig. 2 is the total reflection coefficients of a four-cell parabolic conductivity profile PML absorber, at the normal incident angle, with the original and the revised finite-difference implementations. The theoretical reflection coefficient of the absorber, by ignoring the numerical reflection at media interfaces, is 10^{-7}. It can be seen that the numerical reflection is substantially reduced with the revised finite-difference scheme.

Fig. 3 shows the numerical reflection versus the theoretical reflection at the normal incident angle and at the frequency $f = 1$ GHz, which corresponds to $\lambda = 300\Delta h$, for a four-cell PML absorber of different conductivity profiles. The conductivity profile of PML is expressed as $\sigma_x = \sigma_m(x/\delta)^n$ and the theoretical reflection coefficient $R_{\rm th}$ relates to the coefficient σ_m and the exponent n by

$$\sigma_m = -(n+1)/(2\delta\eta)\ln R_{\rm th}. \tag{11}$$

As can be seen from Fig. 3, when $R_{\rm th}$ is relatively large (or σ_m is small), the reflection of the original and the revised schemes are about the same. This is because, for these cases, the main reflection from the PML absorber is actually from the electric wall terminating the PML. As $R_{\rm th}$ becomes smaller, the numerical reflection from medium interfaces becomes a more significant part of the total reflection, and the improve-

$$R_e = -\frac{\frac{2j(\hat{\epsilon}-\epsilon)}{\Delta t}\sin\frac{\omega\Delta t}{2} + \left[\hat{\sigma}_x - \frac{\sigma_{1x}+\sigma_{2x}}{2}\right]\cos\frac{\omega\Delta t}{2} + \frac{1}{Z\Delta h}\left[\cos\frac{k_{2x}\Delta h}{2} - \cos\frac{k_{1x}\Delta h}{2}\right]}{\frac{2j(\hat{\epsilon}-\epsilon)}{\Delta t}\sin\frac{\omega\Delta t}{2} + \left[\hat{\sigma}_x - \frac{\sigma_{1x}+\sigma_{2x}}{2}\right]\cos\frac{\omega\Delta t}{2} + \frac{1}{Z\Delta h}\left[\cos\frac{k_{2x}\Delta h}{2} + \cos\frac{k_{1x}\Delta h}{2}\right]} \tag{3}$$

$$R_e^r = -\frac{\frac{2j(\hat{\epsilon}-\epsilon)}{\Delta t}\sin\frac{\omega\Delta t}{2} + \left[\hat{\sigma}_x - \frac{\sigma_{1x}+\sigma_{2x}}{2}\right]\cos\frac{\omega\Delta t}{2} - \frac{1}{Z\Delta h}\left[\cos\frac{k_{2x}\Delta h}{2} - \cos\frac{k_{1x}\Delta h}{2}\right]}{\frac{2j(\hat{\epsilon}-\epsilon)}{\Delta t}\sin\frac{\omega\Delta t}{2} + \left[\hat{\sigma}_x - \frac{\sigma_{1x}+\sigma_{2x}}{2}\right]\cos\frac{\omega\Delta t}{2} + \frac{1}{Z\Delta h}\left[\cos\frac{k_{2x}\Delta h}{2} + \cos\frac{k_{1x}\Delta h}{2}\right]} \tag{5}$$

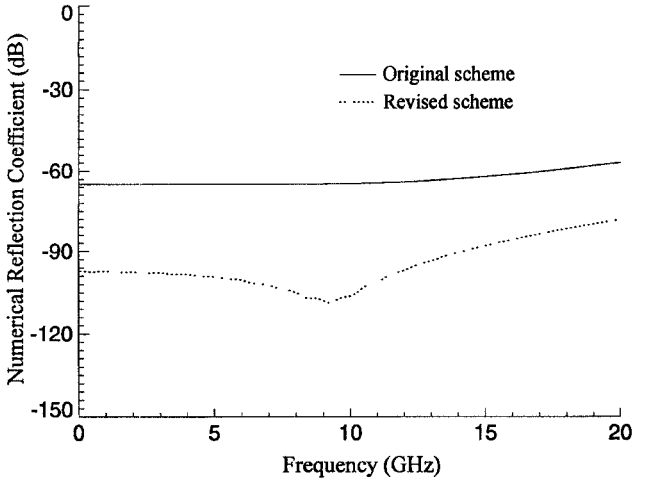

Fig. 2. Numerical reflection coefficient for a four-cell PML absorber with the original and the revised finite-difference equations.

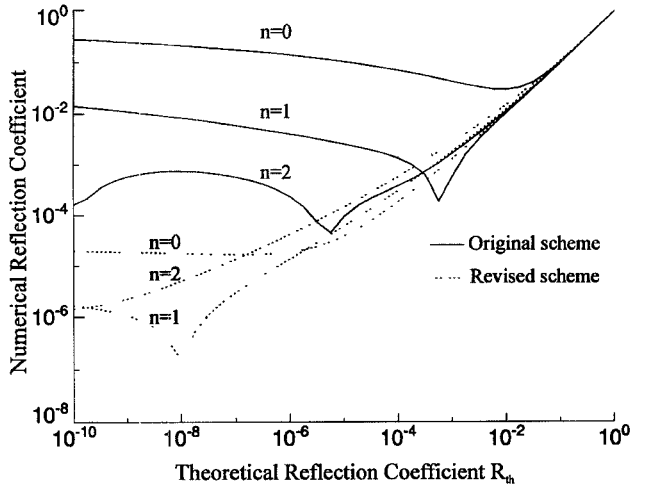

Fig. 3. Comparison of numerical reflection coefficients of the original and the revised schemes for a four-cell PML of different conductivity profiles.

ment by the revised finite-difference scheme is more apparent. It can be seen from Fig. 3 that for a PML of the same thickness and the same conductivity profile, the minimum obtainable reflection coefficient of the revised finite-difference scheme can be a few orders of magnitude smaller than that of the original scheme.

Fig. 4 is the reflection coefficient versus the incident angle, at the frequency corresponding to $\lambda = 100\Delta h$, for a four-cell PML absorber of constant conductivity profile and the theoretical reflection coefficient of 10^{-5}. As can be seen, the best absorption of the revised finite-difference equation depends on the angle θ chosen. Even when θ is chosen to be

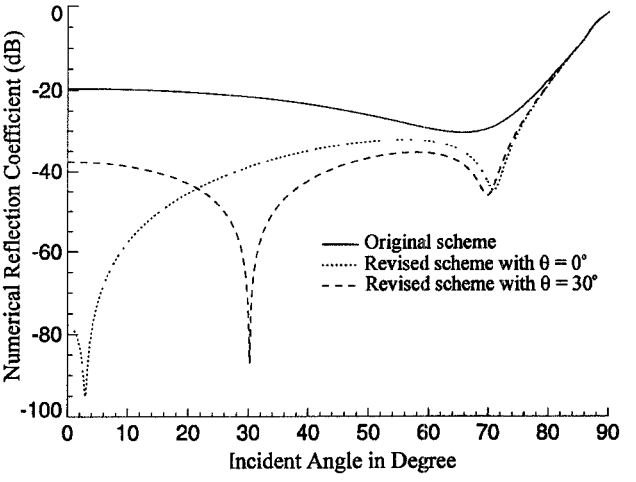

Fig. 4. Numerical reflection coefficient versus incident angle for the original and the revised schemes. The PML absorber has a constant conductivity profile and a theoretical reflection coefficient of 10^{-5}.

zero, the improvement on the reduction of numerical reflection by the revised finite-difference equation appears in a large range of incident angles.

Numerical tests have also been performed on PML's for terminating waveguide structures. Significant reduction in numerical reflection is also achieved with the revised finite-difference scheme.

IV. Conclusion

A new finite-difference scheme for the numerical implementation of the PML is developed. With the new algorithm, the numerical reflection of PML can be significantly reduced, which leads to more accurate numerical computation and reduced requirements of computer resources.

References

[1] J. P. Berenger, "A perfectly matched layer for the absorption of electromagnetic waves," *J. Comput. Physics*, vol. 114, pp. 185–200, Oct. 1994.

[2] M. Gribbons, S. K. Lee, and A. C. Cangellaris, "Modification of Berenger's perfectly matched layer for the absorption of electromagnetic waves in layered media," in *Proc. 11th Annu. Rev. Progress in Applied Computational Electromagnetics*, Monterey, CA, Mar. 20–25, 1995, pp. 498–503.

[3] J. Fang and Z. Wu, "Generalized perfectly matched layer—An extension of Berenger's perfectly matched layer boundary condition," *IEEE Microwave Guided Wave Lett.*, pp. 451–453, Dec. 1995.

[4] W. C. Chew and J. M. Jin, "Analysis of perfectly-matched layers using lattice EM theory in a discretized world," in *1995 USNC/URSI Dig. Radio Science Meet.*, Newport Beach, CA, p. 338.

[5] J. Fang and Z. Wu, "Closed form expression of numerical reflection coefficient at PML interfaces and optimization of PML performance," accepted for publication in *IEEE Microwave Guided Wave Lett.*